frontiers
in Oncology

Nanozymes in Tumor Theranostics

Qiulian Ma[1†], Yanfang Liu[2†], Haitao Zhu[1*], Lirong Zhang[1*] and Xiang Liao[1,3*]

[1] Department of Medical Imaging, The Affiliated Hospital of Jiangsu University, Zhenjiang, China, [2] School of Medicine, Jiangsu University, Zhenjiang, China, [3] Department of Laboratory Medicine, The Affiliated Hospital of Jiangsu University, Zhenjiang, China

Nanozymes, a new generation of enzyme mimics, have recently attracted great attention. Nanozymes could catalyze chemical reactions as biological enzymes under physiologically mild conditions with higher-efficiency catalytic activities. Moreover, nanozymes could overcome the shortcomings of natural enzymes, such as easy inactivation, high cost, and low yield. With the development of more and more smart and multi-functional nanosystems, nanozymes display great achievement in tumor biology. In this review, we outline the recent advances of nanozymes in tumor and tumor microenvironment diagnosis, therapy, and theranostics.

Keywords: nanozyme, tumor microenvironment, diagnosis, therapy, theranostics

INTRODUCTION

Despite the great achievement of traditional cancer treatment, such as chemotherapy and immunotherapy, tumors continue to be a major cause of morbidity and mortality. The crosstalk between tumor cells and the tumor microenvironment (TME) is a critical factor for therapy resistance, relapse, and metastasis (1). Therefore, it is important to explore novel strategies to enhance tumor treatment sensitivity by targeting both cancer cells and TME.

Nanomaterials have recently received great interest in enhancing the outcome of cancer therapy, especially nanozymes. Natural enzymes are the proteins or ribonucleic acid (RNA) with highly specific and catalytic ability to their substrates produced by living cells. However, the intrinsic characteristics of natural enzymes, such as storage difficulty, easy deactivation, and high cost, limit their further clinic application (2). With the unexpected discovery of horseradish peroxidase (HRP) activity of Fe_3O_4 magnetic nanoparticles (Fe_3O_4 MNPs) in 2007, the artificial nanozymes that display similar catalytic mechanism and efficiency to natural enzymes gradually become research hotspots (3). Nanozymes were firstly identified as nanomaterials possessing intrinsic enzyme-like activities (3). Recently, with the development of chemistry and biology, nanozymes are now termed inorganic or organic nanomaterials possessing intrinsic enzyme-like catalytic activities with abundant advantageous properties compared to natural enzymes, such as lower cost, more facile preparation, higher operational ability, and multi-functionalization (4–7).

Based on the rapid development of nanotechnology, the majority of nanoparticles, such as magnetic nanomaterials, cerium oxide nanoparticles (nanoceria), carbon nanotubes (CNTs), graphene oxide (GO), and gold nanoparticles (Au NPs), have demonstrated their intrinsic redox catalytic activities (3, 8–16). Due to the unique properties of nanozymes and the specific characteristics of tumor and TME, deeper and wider applications of nanozymes in tumor diagnosis, therapy, and theranostics are becoming more and more possible. In this review, we firstly briefly summarize the classification of the most common nanozymes and then discuss the promising applications and challenges of nanozymes in the field of tumor theranostics.

CLASSIFICATION OF NANOZYMES

Nanozymes mainly include the following subtypes: peroxidase (POD), oxidase (OXD), catalase (CAT), and superoxide dismutase (SOD) (**Figure 1**). More importantly, great efforts must be devoted to the exploration of novel nanozymes. In this section, we discuss only a few parts of representative nanozymes based on their compositions.

Carbon-Based Nanozymes

Carbon-based nanomaterials, including carbon nanotubes (CNTs), graphene oxide (GO), carbon nanospheres, and carbon nanodots (C-Dots), have been proved as the POD mimic catalytic enzyme (11, 15, 17–23), while fullerene and its derivatives perform the SOD-like activity (4).

Combining the ability of hemin to catalyze various oxidation reactions and the large open surface area and rich surface chemistry of graphene, the nanoplatform-modified hemin onto the surface of graphene through the π–π stacking can serve as POD enzymes and display stable geometric support and efficient molecular loading ability (19, 20).
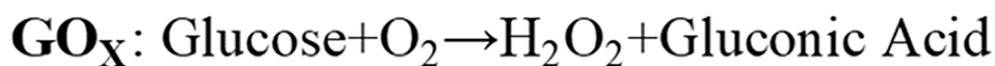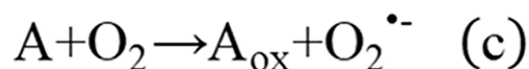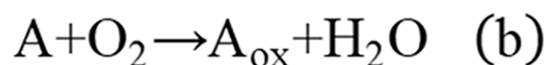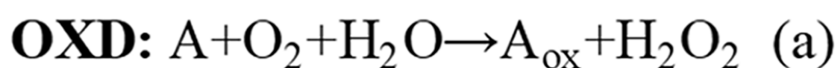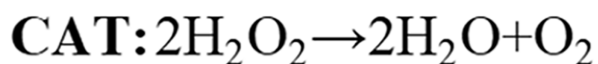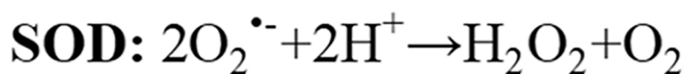
The carboxyl-modified graphene oxide (GO-COOH) with the intrinsic POD property could catalyze the peroxidase substrate 3,3',5,5'-tetramethylbenzidine (TMB) in the presence of hydrogen peroxide (H_2O_2) (15). The accompanying blue color reaction makes them capable to be developed for a cheaper and more sensitive glucose detection (15).

CNTs can be distinguished as single-wall carbon nanotubes (SWNTs) and multi-wall carbon nanotubes (MWNTs) according to the number of graphene layers (24). SWNTs could catalyze the substrate of TMB, which have been developed to target dsDNA efficiently (11). Moreover, it has been confirmed that the enzymatic activity of carbon nanotubes strongly depended on pH, temperature, and H_2O_2 concentration (11).

Based on the superior enzyme activities of nitrogen-doped carbon nanomaterials (N-CNMs), N-doped porous carbon nanospheres (N-PCNSs) possess excellent mimic activities, including OXD-, POD-, CAT-, and POD-like activities (25). These activities are positively correlated with the concentration of N dopant and can also be tunable by pH and temperature (25, 26). Additionally, the B/Fe-doped carbon nanoparticles can also function as POD catalysts (26, 27).

Metal-Based Nanozymes

With the high glucose conversion ability, gold nanoparticles (Au NPs) have been discovered to perform POD- and OXD-like activities (13, 14). Mesoporous silica nanoparticles (MSN) or bovine serum albumin (BSA) can be assembled on the surface of Au NPs for the detection of glucose or dopamine (DA) by the distinguished GOx- and POD-like activities of Au NPs (28, 29). However, high temperature can result in the poor catalytic performance of Au NPs due to the instability of enzymatic product $ABTS^{\bullet+}$, which can be improved by ionic liquid (30).

$$\text{SOD: } 2O_2^{\bullet-} + 2H^+ \rightarrow H_2O_2 + O_2$$

$$\text{CAT: } 2H_2O_2 \rightarrow 2H_2O + O_2$$

$$\text{POD: } 2AH + H_2O_2 \rightarrow 2A + 2H_2O$$

$$\text{OXD: } A + O_2 + H_2O \rightarrow A_{ox} + H_2O_2 \quad (a)$$

$$A + O_2 \rightarrow A_{ox} + H_2O \quad (b)$$

$$A + O_2 \rightarrow A_{ox} + O_2^{\bullet-} \quad (c)$$

$$\text{GO}_X\text{: Glucose} + O_2 \rightarrow H_2O_2 + \text{Gluconic Acid}$$

FIGURE 1 | Nanozyme reaction formulas.

The stable platinum nanoparticles (Pt NPs) have the ability to scavenge H_2O_2, superoxide anion (O_2^-), and singlet oxygen ($^1O_2$), simulating CAT-, SOD-, and OXD-like activities. The specific catalytic enzyme activities of Pt NPs are tightly dependent on temperature and pH [31, 32]. Under the low pH environment, Pt NPs mostly possess POD-like activity, while Pt NPs exhibit CAT- and SOD-like activities under neutral conditions [31, 32]. Moreover, there is a positive correlation between enzyme activities and Pt content. Escapsulating apo-ferritin on the Pt NPs (PtNP@apo-ferritin), this system exhibited more outstanding SOD-like activity and longer-term stability [32, 33].

Metal Oxide-Based Nanozymes

Nanoceria and iron oxide magnetic nanoparticles (Fe_3O_4 MNPs) are the most widely utilized metal oxide catalysts among the metal oxide-based nanomaterials [5, 8–10, 16, 34, 35]. Nanoceria exists in a mixed valence state (Ce^{3+} and Ce^{4+}) [9, 36–38]. The ratio of Ce^{3+} and Ce^{4+} determines the catalytic enzyme activity of nanoceria. Nanoceria mainly performs SOD-like activity with a high Ce^{3+}/Ce^{4+} ratio, while performing CAT-mimic activity with a low Ce^{3+}/Ce^{4+} ratio [7]. Moreover, the activity of nanoceria and Fe_3O_4 MNPs can be controlled by pH. Under the low pH environment, nanoceria possesses an intrinsic OXD-like activity [9]. Fe_3O_4 MNPs display a POD-like activity under acid conditions, while showing CAT-like activity in a neutral environment through the decomposed H_2O_2 [39–41]. The manganic oxide nanoparticles (MnO NPs) behave as the SOD, CAT, and GOx enzymes, inducing the elimination of hydroxyl radical (·OH), maintaining redox homeostasis, and protecting cells from neurotoxin-induced damage [42].

Metal Chalcogenide Nanozymes

Copper monosulfide (CuS) nanoparticles (CuS NPs) have been demonstrated to perform POD-mimic activity by catalyzing the peroxide substrate 3,3',5,5'-TMB in the presence of H_2O_2 [43–47]. Moreover, with the CuS NPs further covered on the graphene, the CuS-graphene nanosheets (CuS-GNSs) possess higher intrinsic POD- and GOx-like activity than CuS or graphene, respectively, which have been employed to detect H_2O_2 concentration and monitor the human blood glucose level [44]. CuS concave polyhedral superstructures (CuS CPSs) possess superior POD-like activity compared to either the initial formed spherical CuS superstructures or convex CuS microspheres, due to the fact that the concave structures constructed by the thinner nanoplates have a hollow/porous structure that led to a higher surface area [43, 48].

It has been proved that several iron chalcogenides can serve as POD-mimic enzymes. FeS_2 nanosheets (FeS_2 NSs) possess the ability to oxidate the peroxide substrate TMB due to the Fe ion located in the active site [49]. Simultaneously, the peroxidase activity of FeS_2 NSs can be tunable by pH and temperature [49]. The FeS_2/SiO_2 double mesoporous hollow spheres (DMHSs) not only exhibit a more outstanding POD-like activity than both Fe_3O_4 NPs and FeS_2 NSs, but also are more susceptive to the detection of H_2O_2 and glutathione (GSH) [50]. The sulfur vacancies in magnetic greigite (SVs-Fe3S4) NSs have demonstrated a distinguished POD-mimic activity resulting from the abundant SVs, which have been developed for the colorimetric detection of glucose in human serum [51].

The MoS_2 nanosheets have been developed for the regulation of oxidation stress due to their intrinsic multi-enzyme-like activities under physiological conditions, including SOD-, CAT-, and POD-mimicking activities [52]. MoS_2 nanosheets can efficiently remove several kinds of reactive oxygen species (ROS) through the Mo^{6+}/Mo^{4+} redox couple and accelerate the electron transfer between TMB and H_2O_2 [52].

The reason why nanozymes are considered to have enzyme-like catalytic activities is that they own high catalytic activities and can catalyze the same chemical reactions as biological enzymes. In addition, compared to biological enzymes, nanozymes have superior biocompatibility, stability, and targeting ability, and play corresponding catalytic activities in different environments. The application of nanozymes in tumor diagnosis and treatment depends on their closer integration of nanotechnology and biomedicine for the.

NANOZYMES IN TUMOR DIAGNOSIS, THERAPY, AND THERANOSTICS

Solid tumors consist of cancer cells and their living environment, also termed tumor microenvironment (TME). Previously, traditional cancer therapy avenues were mostly focused on cancer cells. Recently, more and more lines of evidence have uncovered that the TME is also critical on tumor malignant behaviors. Therefore, targeting both cancer cells and TME is becoming a promising cancer therapy method. TME includes the various soluble substance and stromal cells, such as fibroblasts, immune and inflammatory cells, glial cells, and other cells, as well as nearby micro-vessels and various biological signal molecules [53, 54]. The "interactive cooperation" between stromal cells and cancer cells facilitates the progression of tumor and contributes to the dramatic dynamic changes and the heterogeneity of TME [53]. In addition, cancer cells could also remodel the TME, ultimately resulting in the immune escape, metastasis, and even relapse of tumor [55]. The characterized metabolism manner, rapid growth, and strong reproduction ability of cancer cells determine their higher demands for oxygen and glucose than normal cells. Cancer cells compete with stromal cells to take advantage of glucose for aerobic glycolysis. Also, abundant lactic acid secreted into the extracellular environment ultimately forms the acid and immunosuppressed TME [56–58]. The broken balance between oxygen consumption and supply resulted in the messy growth and irregular distribution of tumor vasculature systems, which, in turn, eventually enhanced the degree of permanent or temporary hypoxia and further increased the osmotic pressure of TME [59]. Therefore, low pH, hypoxia, excessive H_2O_2 and GSH, high osmotic pressure, and immunosuppressive microenvironment are the outstanding hallmarks of solid tumors (**Figure 2**) [53, 56, 58]. These characteristics are mutually causal, finally contributing to the rapid progression of tumor. Targeting and normalizing TME seem to be a new and

FIGURE 2 | The characteristic of tumor microenvironment.
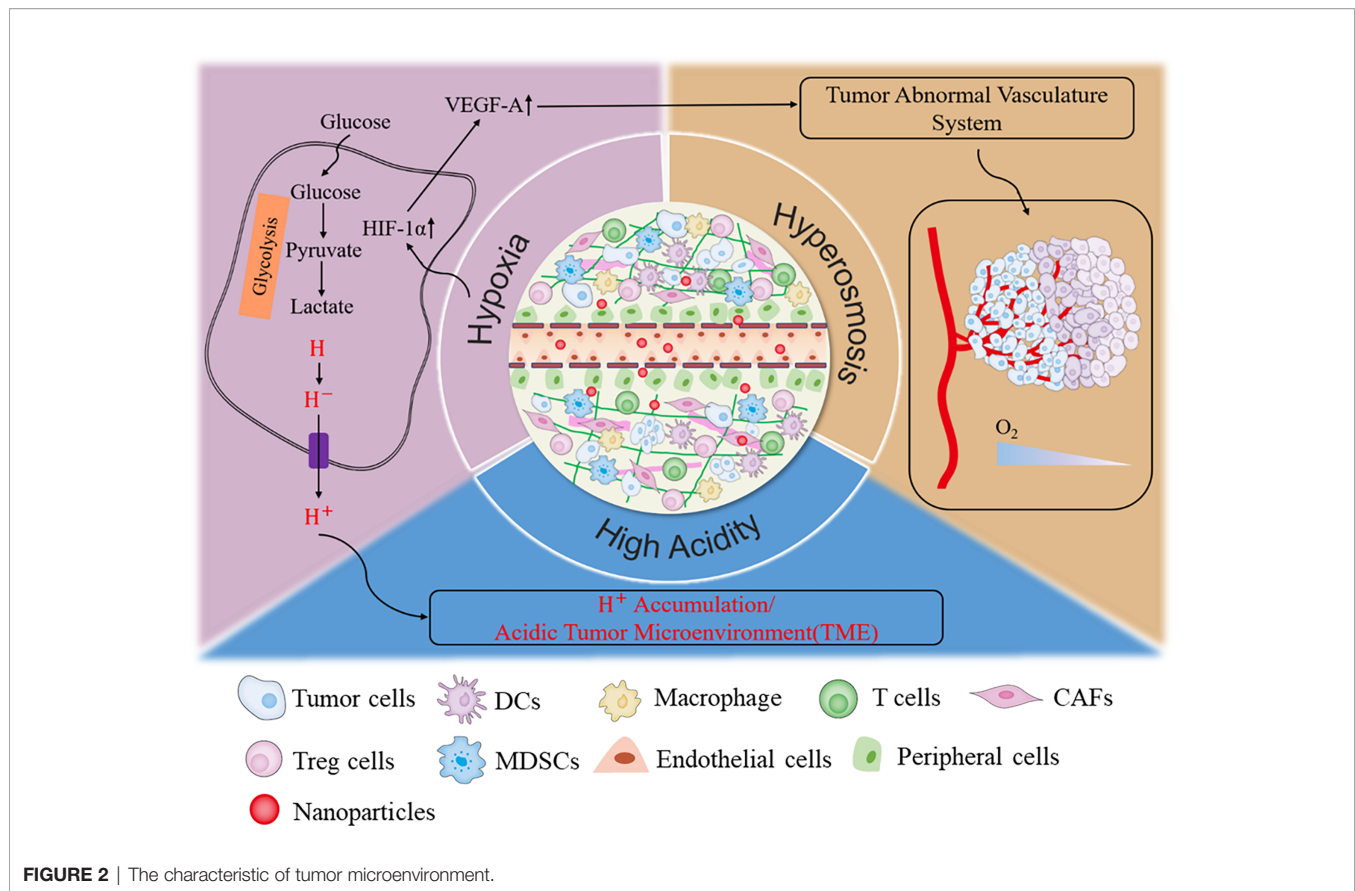
effective method for tumor diagnosis and treatment. Recently, more and more nanozymes have been constructed to target the diagnosis and treatment of TME.

Nanozymes in Tumor Cells and Tumor Microenvironment Target Diagnosis

Nanotechnology-based tumor target diagnosis and therapy include passive target and active target. Active target greatly relies on the recognition of the specific receptors overexpressed on cancer cells and the ligand-directed binding on the surface of nanosystems (60). Loaded with special markers on the cancer cell surface, such as transferrin, growth factors, peptides, folate, antibodies, or antibody fragments, nanozyme systems not only recognize tumor more sensitively, but also result in drug delivery more specifically (61). The nanozymes modified with folic acid can actively target the folic acid receptors on the cancer cell surface and further can serve as oxidants to promote cancer cell death (9, 17). Porous platinum nanoparticles on graphene oxide (Pt NPs/GO) can function as peroxidase mimetics. which enable them to detect cancer cells by the color reaction of TMB (62). Furthermore, by loading folic acid on the Pt NPs/GO, this nanosystem can distinguish a total of 125 cancer cells more broadly than naked-eye observation (62). Prostate-specific antigen (PSA), a special tumor biomarker, can be attached by the immune complexes based on the intrinsic POD-like activity of GO, and then the PSA concentration could be directly

detected with the colorimetric reaction (63). Ultra-small gold nanoclusters (Au NCs) can serve as POD-like catalysts for disproportionation and decomposition of H_2O_2, which make them sensitive probes for tumor imaging *in vivo* (64). The multifunctional protease nanosensor constructed by Au NCS not only can determine whether the tissue is cancerous through the catalyzed reaction of Au NCS according to the color reaction, but also is non-toxic and can be completely eliminated by liver and kidney excretion (64). Furthermore, the magneto-ferritin nanoparticles (M-HFn) are composed of iron oxide and heavy-chain ferritin (HFn) shell (65). Due to the ability of targeting transferrin receptor 1 (TfR1) overexpressed on cancer cell surface and the color reaction in tumor site resulting from the POD-like activity of the iron oxide core that could catalyze the abundant H_2O_2 in TME, M-HFn could visualize cancer tissues sensitively and specifically (65). Similarly, HFn-N-PCNSs-3 can also specifically identify the cancer cells and effectively reduce the tumor volume dependent on the special binding of TfR1 on cancer cell surface and the multi-enzyme mimic activities of N-PCNSs-3 (25). Besides, angiopep-2, a specific ligand of lipoprotein related protein-1 (LRP1), anchored on the surface of Au NPs can penetrate through the blood–brain barrier (BBB) and further actively target glioma cancer cells (66, 67).

Magnetic resonance imaging (MRI) contrast agents based on the ROS-stimulated responses, such as superoxide ions, H_2O_2, and hydroxyl radicals, have been promising tumor diagnostic

and imaging markers due to their extensive accumulation and persistent presence in TME (68–70). Prussian Blue nanoparticles (PBNPs, $KFe^{3+}[Fe^{2+}(CN)_6]$) perform CAT-like activities under the neutral pH condition (71). The core Fe^{3+} with water coordination can form paramagnetic oxygen bubbles, which are conducive to shorten the MRI T1-weighted image (T1WI) relaxation time and then enhance the MRI contrast (72). Based on the previous pioneering work of PBNPs, SPIO@GCS/acryl/biotin-CAT/SOD-gel (SGC), a dual-enzyme-loaded multifunctional hybrid nanogel probe, has been developed to strengthen the ultrasound imaging and the imaging contrast of T2WI (73). In recent years, the PB@Au core-satellite nanoparticles (CSNPs) have been constructed to explore multiple diagnostic and therapeutic strategies of tumors (72). CSNPs can achieve dual-model imaging due to the PB NPs that acted as MRI T1WI contrast agents and the enhanced computed tomography (CT) imaging efficiency by AuNPs (72). Besides, the MnO NPs exposed to the superoxide radicals could enhance the MRI signal and simultaneously treat the catalytic-induced tumor progression due to their intrinsic SOD-mimic ability (74). Moreover, the CAT-like nanoparticles are gradually utilized as coupling or contrast agents of ultrasound (US) and MRI owing to the enhanced catalyzed H_2O_2 into O_2 molecules (71–73).

Early diagnosis of tumor makes it possible to obtain outstanding tumor clearance and satisfactory clinical prognosis by local treatment. Nowadays, the early detection of tumor mainly depends on the blood tumor markers and imaging manifestations. However, the extremely low abscission rate of early tumor markers or the lack of specificity of imaging findings limits the accuracy and sensitivity of early tumor detection in clinical. The emergence of nanozymes provides new ideas and methods for the early diagnosis of tumor and the visualization of tumor tissues, which greatly improve the specificity and sensitivity of early diagnosis of tumor.

Nanozymes in Synergistic Tumor Therapy

Nanozymes can achieve anti-tumor effects by improving TME. For example, the highly ordered $MnO_2@PtCo$ nanoflowers are developed as a ROS generation nanoplatform for tumor therapy by targeting the hypoxia and the acidic pH of TME (75, 76). Cooperating with the OXD-like activity of PtCo and the CAT-like activity of MnO_2, the $MnO_2@PtCo$ nanozymes not only could supply O_2 to overcome the hypoxic TME, but also catalyze ROS formation, which further induces the admirable tumor apoptosis (75). Similarly, the $DMSN-Au-Fe_3O_4$ composited nanoplatforms could make the TME-responsive tumor vanish owing to the GOx-mimic activity of Au NPs and the POD-like activity of the Fe_3O_4 nanoparticles. The $DMSN-Au-Fe_3O_4$ nanozymes are capable of catalyzing β-D-glucose oxidated into gluconic acid and subsequently produce high-toxic hydroxyl radicals for tumor regression (41). Based on the abundant GSH detained in TME, pyrite nanozymes and FeS_2 with ultrahigh H_2O_2 affinity promote the glutathione oxidation due to their OXD-like activity and the generation of •OH by their POD-like activity, resulting in the ferroptosis and apoptosis of tumor cells consequently (35). Recently, a novel nanosystem,

polyethylene glycol (PEG)-ylated iron manganese silicate nanoparticles (IMSN) loaded with TGF-β inhibitor (TI) (IMSN-PEG-TI), has also been constructed to regulate the tumor immune microenvironment and advance the tumor therapeutic modality through the intrinsic POD- and CAT-like activities of IMSN nanozymes under the acidic TME (58).

Additionally, nanozymes can synergistically enhance the anti-tumor effects of tumor therapy avenues that deeply depend on the oxygen level, such as photodynamic therapy (PDT), photothermal therapy (PTT), sonodynamic therapy (SDT), radiotherapy (RT), and chemotherapy (1, 77). Moreover, consumption of O_2 and tumor vasoconstriction can further exacerbate hypoxia and limit the efficiency of the above tumor therapies, which finally form a positive feedback (78–81). Nanozymes are used more and more widely in enhancing the efficiency of these therapies.

Nanozymes in Synergistic Phototherapy

Phototherapy relies on light radiation to induce the death of cancer cells, including PDT and PTT. PDT firstly transforms light energy to the surrounding O_2 and then produces a high concentration of cytotoxicity of ROS to further oxidize biomacromolecules and induces their dysfunction (77, 82–84). PTT induces the death of tumor cells depending on the local thermal damage (77, 84, 85). Although the photosensitizers and photothermal agents could enhance therapy efficiency and reduce the side effect of PDT and PTT under near-infrared (NIR) laser irradiation, they convert to excited single states and then return to the ground states by collisions between surrounding molecules. Accompanied by the increased kinetic energy, they consequently result in the heating of the surrounding microenvironment (77, 85).

Although the metal-organic frameworks (MOFs) assembled with photosensitizers can induce the death of tumor cells by the conversion of oxygen into $^1O_2$, the efficiency of PDT is still limited owing to the hypoxia of the TME (80, 81, 86). The novel Pt nanozymes have been placed on the photosensitizers integrated with MOFs to break the limitation of hypoxia. This nanoplatform not only possesses higher stability, but also performs CAT-like activity leading to the additional $^1O_2$ formation and further enhancing the efficiency of PDT (81).

CAT-mimicking Pt NPs are sandwiched into the dual-nanozyme-engineered porphyrin metal organic frameworks (PCN); furthermore, the outer GOx-mimicking Au NPs coordinate with folic acid (Pt@P-Au-FA) (87). The Pt@P-Au-FA NPs can enhance O_2 generation by catalyzing H_2O_2, which further enhances PDT efficiency. What is more, Au NPs strengthen the depletion of glucose and the self-produced H_2O_2 serve as substrates of Pt NPs, cooperating with glucose depletion-induced starving therapy and achieving remarkable anti-tumor effects (87).

The nanozyme PEG/Ce-Bi@DMSN is constructed by dendritic mesoporous silica coated with uniform Bi_2S_3 nanorods (Bi_2S_3@DMSN) and further by ultrasmall ceria placed into the large mesopores of Bi_2S_3@DMSN, which possesses dual mimic catalytic activities (including POD- and CAT-mimic activities) under primary acidic TME resulting in

elevated oxidative stress and relieved hypoxia (88) (**Figure 3**). Additionally, PEG/Ce-Bi@DMSN allowed the enhanced GSH consumption to be overexpressed in TME. The NIR laser irradiation could strengthen the catalytic activities and GSH depletion of PEG/Ce-Bi@DMSN nanozymes, which further synergistically enhance the tumor ablation effect of PTT (88).
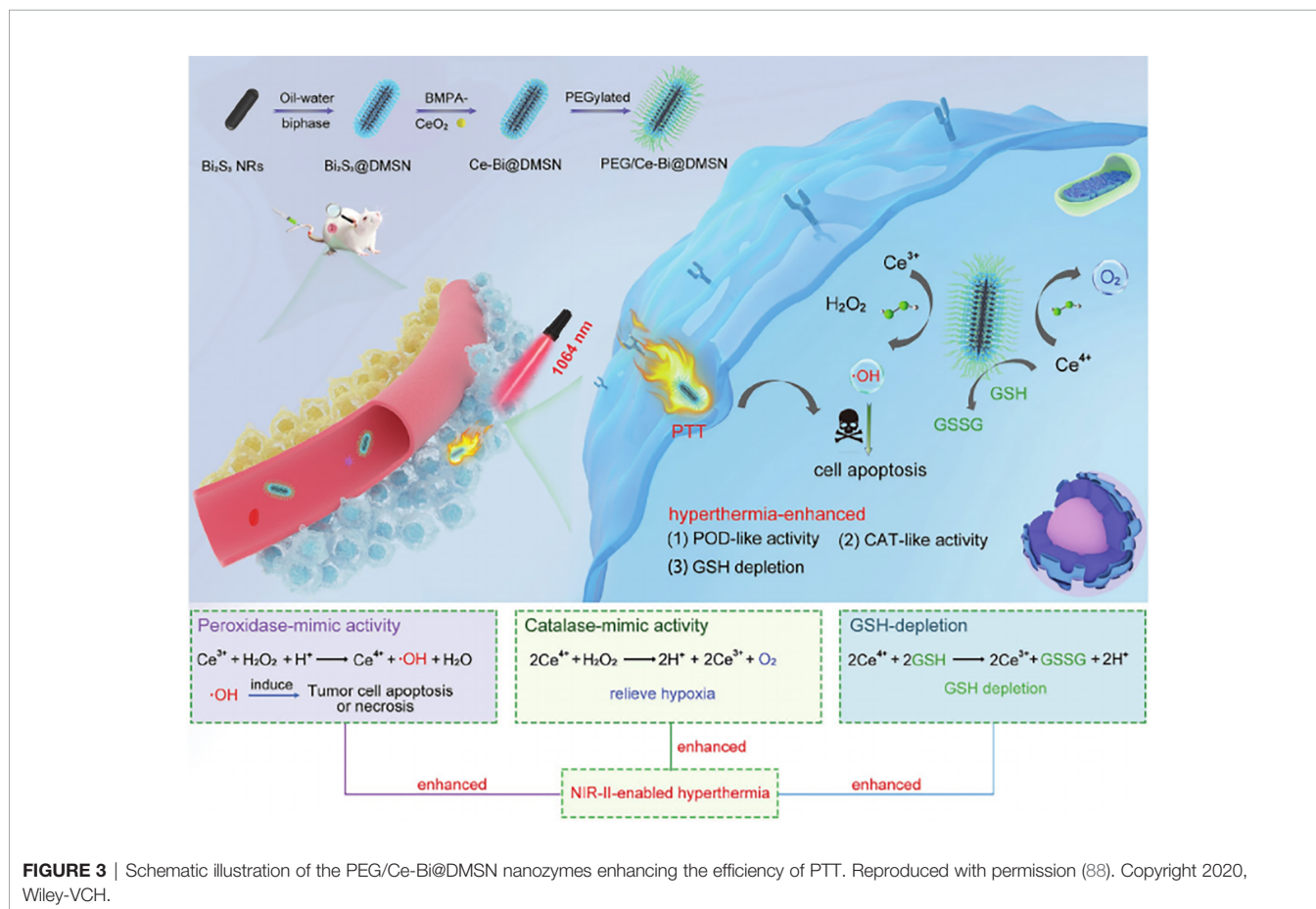
The platinum-doped Prussian blue (PtPB) nanozyme was developed to improve the photothermal property in a large wavelength range during the process of PTT (89). On the other hand, the PtPB nanozyme is endowed with superior CAT and SOD-like catalytic activities by Pt doped with PB nanotubes, which contributed to the relieved inflammation caused by PTT, along with significant tumor inhibition (89).

Nanozymes in Synergistic Sonodynamic Therapy

Ultrasound (US)-triggered sonodynamic therapy (SDT) consisting of a low-intensity ultrasound and a chemotherapeutic agent (sonosensitizer) is a promising alternative tumor therapeutic modality (90–93). US not only is more accessible and noninvasive in reaching deep-seated tumor tissues, but also can activate sonosensitizers to produce toxic ROS molecules for tumor eradication (90, 91, 94). However, the therapeutic efficiency of SDT is still restricted by severe hypoxia in TME to a great extent (90, 95).

The hollow Pt-CuS Janus can overcome the hypoxia environment due to the mimetic enzyme activity of Pt that decomposes the endogenous overexpressed H_2O_2 into O_2 (47). The hollow Pt-CuS Janus has superior photothermal performance, which not only elevates the Pt enzyme activity for O_2 production, but also augments the SDT-induced tumor cell death by higher ROS level simultaneously (47). Hence, the synergistic efficiency of PTT and the catalysis-improved SDT can achieve complete tumor elimination.

The nanoprobe (CDP@HP-T), constructed by Pt-embedded hollow polydopamine (P@HP) nanoparticle, co-loaded with doxorubicin (DOX) and chlorine e6 (Ce6) and further modified with the mitochondrial-targeting molecule triphenyl phosphonium (TPP), can be used to achieve enhanced combination therapy of chemotherapy and SDT for tumors (94). As a pH-responsive nanoprobe, the CDP@HP-T could realize the abundant O_2 generation and alleviate the hypoxia of tumor sites responsible for the CAT-like activity of Pt and endogenous overexpressed H2O2 under weakly acidic TME, which further enhances the efficacy of SDT (94). Concomitantly, with DOX and TPP, this nanoprobe could achieve tumor eradication by inhibiting cellular DNA replication, further enhancing the combined therapeutic efficacy of chemotherapy and SDT (94).

FIGURE 3 | Schematic illustration of the PEG/Ce-Bi@DMSN nanozymes enhancing the efficiency of PTT. Reproduced with permission (88). Copyright 2020, Wiley-VCH.

Analogously, the ultrafine titanium monoxide (TiO_{1+x}) nanorods modified with PEG (PEG-TiO_{1+x} NRs) enable higher tumor elimination outcome in synergistic chemotherapy and SDT (**Figure 4**) (96). The TiO_{1+x} NRs possess POD-like activity for the decomposition of H_2O_2 in TME (96). Notably, the PEG-TiO_{1+x} NRs could generate superior US-induced ROS due to the oxygen-deficient structures within TiO. On the other hand, the PEG-TiO_{1+x} NRs could serve as Fenton-like agents for ROS generation in the presence of Ti^{3+} (96).

Nanozymes in Synergistic Radiotherapy

Radiotherapy (RT) has been widely used as the first-line treatment modality of various solid tumors in clinics (97–101). However, the TME complex leads to the ultimate resistance to RT and even the recurrence and metastasis of tumors (98). Normalizing the TME to enhance the effectiveness of RT, to improve hypoxia and increase intratumoral oxygen concentration, and to further promote radiation-induced DNA damage is one of the most common strategies.

Several nanomaterials are designed to enhance tumor radiation sensitivity and attenuate hypoxia by catalyzing the generation of O_2 (102, 103). The high reactivity, stability, and specificity of the albumin complex and MnO_2 NPs (A-MnO_2 NPs) towards H_2O_2 could simultaneously modulate hypoxia and acidosis TME with regulated pH (102). Furthermore, A-MnO_2 NPs could normalize tumor blood vessels by the downregulated hypoxia-inducible factor-1α (HIF-1α) and vascular endothelial growth factor (VEGF) (102). Taking advantage of the engineered multifunctional A-MnO_2 NPs, the tumor response to radiation can be enhanced significantly (102).

Based on the perfect RT responsiveness of MnO_2, gold and manganese dioxide (Au@MnO_2) core-shell nanoparticles coated with PEG formed Au@MnO_2-PEG (104). Au@MnO_2-PEG, using the Au core, functioned as a RT sensitizer and MnO_2 shell as CAT mimics that mediate the decomposed H_2O_2 could not only overcome tumor hypoxia but also enhance the tumor sensitivity to RT (75, 104). More importantly, the Au@MnO_2-PEG displays more satisfactory tumor inhibition than the outcome of Au-PEG or MnO_2-PEG and has good biocompatibility and biosecurity (104).

Nanozymes in Synergistic Chemotherapy

Chemotherapy, as the most commonly applied cancer treatment modality, induces cancer cell death partly through regulating the formation of ROS (105). Abundant nanozymes loading chemotherapy drugs have been applied in tumor treatment depending on enhancing the generation of ROS (106).
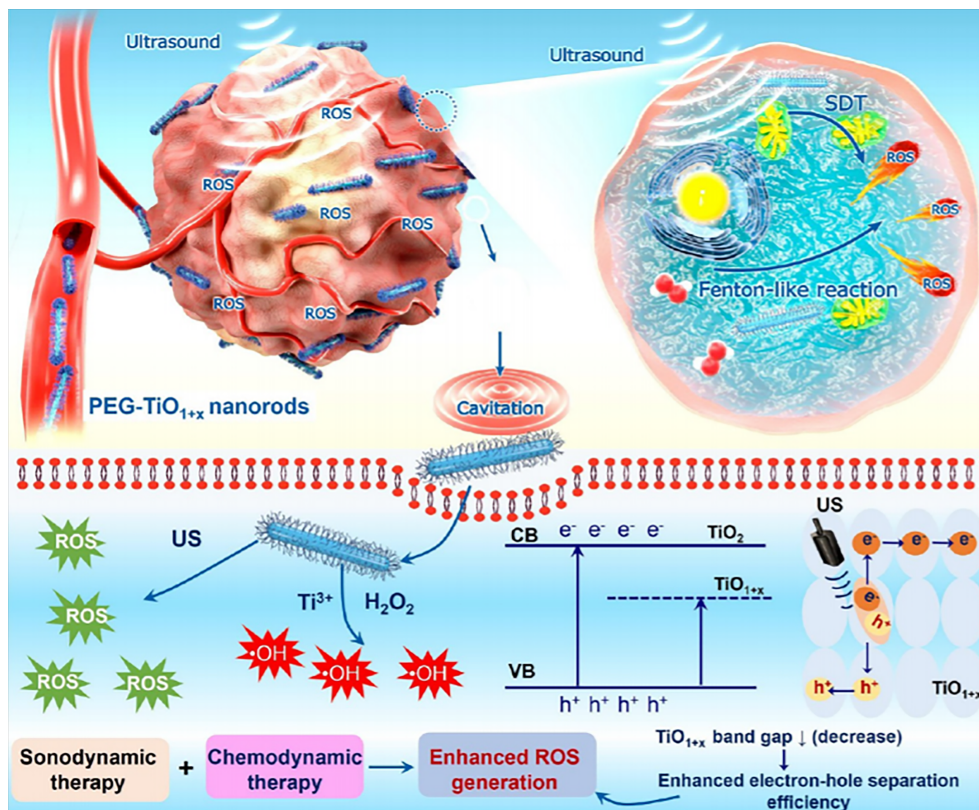
FIGURE 4 | Schematic illustration of PEG-TiO_{1+x} NRs that served as sonosensitizers in the synergistic chemotherapy and SDT. Reproduced with permission (96). Copyright 2020, American Chemical Society.

Iron oxide nanoparticles (IONPs), with the POD-like activity, could decompose H_2O_2 into hydroxyl radicals under acidic or neutral conditions (73). The super-paramagnetic iron oxide nanoparticles (SPION) with inherent POD-like activity are proved to reduce H_2O_2 in human mesenchymal stem cells (hMSCs) in a dose-dependent manner, and further promote cell proliferation and growth (107). SPION can also be degraded in lysozymes and produce iron ions, which further accelerates the process of cell cycle (106). In addition, the combination of SPION with β-lapachone, an anticancer drug, significantly enhances the intracellular ROS levels and tumor-killing efficiency in non-small cell lung cancers (NSCLCs) (106).

TABLE 1 | Nanozyme Classification and Applications.

Nanozyme system	Mimetic activities	Applications	References
Carbon-Based			
SWNTs	POD	Drug delivery; Human SNP DNA detection	(11, 24)
GO	POD	Tumor visual detection	(63)
GO-COOH	GOx; POD	Glucose detection	(15)
GFH	POD	Tumor detection	(17)
C-Dots	POD	Glucose detection	(22)
HFn-N-CNMs-3	POD; OXD (acidic pH values)	Tumor catalytic therapy	(25)
	SOD; CAT (neutral pH values)	Anti-oxidant therapy	(25)
Metal-Based			
Au NPs	GOx	Self-limiting nanomedicine; Biomedical probe	(14, 111)
EMSN-AuNPs	GOx; POD	Self-activated cascade catalysis	(28)
AuNCs	POD	Tumor detection	(64)
BSA-AuNCs	POD	A dual fluorometric and colorimetric sensor for dopamine	(29)
Au/SiO_2 nanocomposites	POD	Realizing high-temperature catalytic reactions	(30)
AuNCs-NH_2	CAT	Enhancing PDT efficiency	(83)
Carbon-gold hybrid nanoprobes	CAT	Real-time imaging, enhancing PTT and PDT efficiency	(111)
Au_2Pt-PEG-Ce6	CAT; POD	Synergistic chemotherapy and phototherapy	(112)
Pt NPs	CAT	Enhancing RT efficiency	(113)
Pt NPs/GO	POD	Tumor detection	(62)
PtPB	CAT; SOD	Enhancing PTT efficiency	(89)
Pt-MOFs hybrid system	CAT	Enhancing PDT efficiency	(81)
Pt-Carbon nanozyme	CAT	Enhancing PDT and PTT efficiency	(84)
P@Pt@P–Au–FA	CAT; GOx	Synergistic starving-like therapy and PDT	(87)
Pd@Pt-T790	CAT	Enhancing SDT efficiency; anti-bacterial infection	(92, 93)
CDP@HP-T	CAT	Synergistic chemotherapy and SDT	(94)
AFeNPs	Fenton reaction	Enhancing MRI contrast and chemotherapy effects	(105)
Fe@BC	POD	Anti-bacterial infection	(27)
Rh-PEG NDs	CAT	Anti-inflammation and anti-tumor	(46)
OxgeMCC-r SAE	CAT	Enhancing PDT efficiency	(114)
IMSN-PEG-TI	POD; CAT	Anti-tumor	(58)
Metal Oxide-Based			
Fe_3O_4 MNPs/IONPs	POD (acidic pH values)	Detection of organophosphorus pesticide and nerve agent	(3, 16, 39)
	CAT (neutral pH values)	Anti-oxidant	(39)
PtFe@Fe_3O_4	POD; CAT	Synergistic tumor catalytic therapy and PTT	(109)
DMSN-Au-Fe_3O_4 NPs	POD; GOx	Anti-tumor	(41)
Nanoceria	SOD (neutral pH values)	Against radiation damage, oxidative stress and inflammation	(9, 10, 38)
		Fluorogenic detection of cancer	
Folate-conjugated Nanoceria	OXD (acidic pH values)	Cancer detection	(9)
PEG-CNPS	SOD	Radical scavenger with tunable redox chemistry	(36)
A-MnO_2 NPs	CAT	Modulating TME and enhancing RT responses	(102)
MnO NPs	SOD	Enhancing MRI contrast	(74)
Au@MnO_2-PEG	CAT	Enhanced RT *via* improving the tumor oxygenation	(104)
Mn_3O_4 NPs	SOD; CAT; GPx	Anti-inflammation	(76)
MnO_2@PtCo	OXD; CAT	Anti-tumor	(75)
rMGB	CAT	Enhancing starvation and PDT against hypoxic tumor	(110)
Ru@CeO_2-RBT/Res-DPEG	CAT	Enhancing dual chemotherapy combined with PTT	(108)
PEG-TiO_{1+x} NRs	POD	Enhancing dual chemotherapy combined with SDT	(96)
Metal Chalcogenide			
CuS-GNSs	POD; GOx	Detection of H_2O_2 and human serum glucose level	(44)
Hollow Pt-CuS Janus	POD	Synergistic PTT and SDT	(47)
DMHSs-FeS_2/SiO_2	POD	Detection of H_2O_2 and GSH for anti-tumor	(50)
SVs-Fe_3S_4	POD	Detection of human serum glucose level	(51)
FeS_2	OXD; POD	Anti-tumor	(35)
PEG/Ce-Bi@DMSN	POD; CAT	Synergistic tumor catalytic therapy and PTT	(88)

Hollow Ru@CeO2 yolk shell nanozymes (Ru@CeO2 YSNs) loaded with anti-tumor drug ruthenium complex (RBT) and resveratrol (Res), and then modified with PEG, formed the Ru@CeO2-RBT/Res-PEG nanozyme system (108). Ru@CeO2-RBT/Res-DPEG could achieve oxygen supply *in situ* and enhance the anti-tumor responses of both chemotherapy and PDT. Moreover, it can also limit the metastasis and recurrence of tumors (108).

Nanozyme Systems for Tumor Theranostics

Based on the development of nanotechnology, more and more multi-functional nanozyme platforms are designed, with the ability of multi-model therapy, multi-model imaging, or simultaneously realizing tumor diagnosis and therapy.

The novel PtFe@Fe$_3$O$_4$ nanozyme, with outstanding POD- and CAT-like activities in the acid TME, could overcome the hypoxia in tumor and enhance the effects of PDT. Moreover, PtFe@Fe$_3$O$_4$ could be used as MRI T1WI negative contrast agents (41, 109). The biomimetic hybrid nanozyme (rMGB), integrated with GOx and MnO$_2$, could realize the self-catalytic reaction products under TME stimulation, resulting in enhanced O$_2$ generation and improving the efficiency of starvation therapy and PDT (110). Also, rMGB could be used as the MRI T1WI contrast agents.

Based on the POD-like and ROS-regulated activity of Au NPs under an acid environment, the carbon–gold hybrid (OMCAPs@rBSA-FA@IR780) nanoprobes not only reveal excellent tumor-targeting imaging ability, but also offer outstanding tumor therapeutic performance (111). Besides, the Au$_2$Pt-PEG-Ce6 nanoplatform was developed through Ce6 linked to Au$_2$Pt nanozymes covalently (112). Contributing to the photosensitive characteristics of Ce6 and the dual CAT- and POD-like activities simultaneously of Au$_2$Pt nanozymes, this nanosystem not only can relieve tumor hypoxia with O$_2$ generation but also enhance the efficiency of PDT and chemotherapy with the produced ·OH (112). Moreover, due to high-Z elements of Au and Pt, Au$_2$Pt-PEG-Ce6 can be possible imaging contrast agents of CT (112, 113).

With single-atom Ru incorporated into the Mn$_3$[Co(CN)$_6$]$_2$ MOF framework, followed by the biocompatible poly-vinylpyrrolidone (PVP) polymer further encapsulating organic ligand, metal ions, and photosensitized Ce6, the self-assembled single-atom enzyme (OxgeMCC-rSAE) was constructed (114). As Ru served as an endogenous oxygen-generating single-atom catalytic site, OxgeMCC-rSAE can degrade H$_2$O$_2$ to generate oxygen, which further enhances the generation of ROS, ultimately enhancing PTT-induced cancer cell death (114). Meanwhile, due to the higher loading of the photosensitizer Ce6, the nanoparticles can selectively aggregate and be visualized in the tumor area by MRI (114).

CONCLUSION AND PROSPECTS

Since the hallmark ferromagnetic nanoparticles proved to be of use as POD natural enzymes in 2007, nanozymes have attracted unprecedented attention and applications, especially in oncology. Although nanozymes have achieved excellent progress in many areas, there are still many problems that cannot be ignored. Currently, most of the present nanozymes mainly focus on the activity of oxidoreductase and hydrolase activities, but the other enzyme activities such as transferase and lyase are still poorly understood. Therefore, it is necessary to explore new nanozyme materials and study their catalytic properties in depth. In addition, the catalytic mechanism of nanozymes is diverse and regulated by various factors. Moreover, different nanozymes may have a synergistic effect in the anti-tumor process. Therefore, it is necessary to establish completeness for different types of nanozyme catalytic systems. The current catalytic efficiency of nanozymes makes it hard to reach the level of natural enzyme *in vivo*, and their activities are still limited due to the complicated TME. Besides, the poor substrate selectivity of nanozymes persists. Modification of certain specific molecules with nanozymes may solve the problem and may improve the substrate specificity and target the tumor more sensitively and specifically. In addition, studies of nanozymes in tumor theranostics are still in the primary stage. The inherent toxicity and clearance rate of the materials also limit their wide applications. Moreover, various nanozymes have their own unique advantages and shortcomings. Therefore, constructing a nanosystem with good biocompatibility, high targeting efficiency, and multiple functions would be a crucial task.

With the continuous development of nanoscale science and technology, nanozymes show superior versatility, operability, and applicability, thus paving the way for new principles and technologies in disease diagnosis and treatment as well as efficient and precise new nanodrug applications in the biomedical field (**Table 1**).

AUTHOR CONTRIBUTIONS

QM and YL wrote the draft of the manuscript. HZ and LZ contributed to the conception of the work and organized the structure of the manuscript. XL performed the revision. All authors contributed to the article and approved the submitted version.

FUNDING

REFERENCES

1. Barker HE, Paget JT, Khan AA, Harrington KJ. The Tumour Microenvironment After Radiotherapy: Mechanisms of Resistance and Recurrence. *Nat Rev Cancer* (2015) 15(7):409–25. doi: 10.1038/nrc3958

2. Liang MM, Yan XY. Nanozymes: From New Concepts, Mechanisms, and Standards to Applications. *Acc Chem Res* (2019) 52(8):2190–200. doi: 10.1021/acs.accounts.9b00140

3. Gao L, Zhuang J, Nie L, Zhang J, Zhang Y, Gu N, et al. Intrinsic Peroxidase-Like Activity of Ferromagnetic Nanoparticles. *Nat Nanotechnol* (2007) 2(9):577–83. doi: 10.1038/nnano.2007.260

4. Wei H, Wang EK. Nanomaterials With Enzyme-Like Characteristics (Nanozymes): Next-Generation Artificial Enzymes. *Chem Soc Rev* (2013) 42(14):6060–93. doi: 10.1039/c3cs35486e

5. Lin YH, Ren JS, Qu XG. Nano-Gold as Artificial Enzymes: Hidden Talents. *Adv Mater* (2014) 26(25):4200–17. doi: 10.1002/adma.201400238

6. Jiang B, Duan DM, Gao LZ, Zhou MJ, Fan KL, Tang Y, et al. Standardized Assays for Determining the Catalytic Activity and Kinetics of Peroxidase-Like Nanozymes. *Nat Protoc* (2018) 13(7):1506–20. doi: 10.1038/s41596-018-0001-1

7. Wu JJX, Wang XY, Wang Q, Lou ZP, Li SR, Zhu YY, et al. Nanomaterials With Enzyme-Like Characteristics (Nanozymes): Next-Generation Artificial Enzymes (II). *Chem Soc Rev* (2019) 48(4):1004–76. doi: 10.1039/c8cs00457a

8. Park KS, Kim MI, Cho DY, Park HG. Label-Free Colorimetric Detection of Nucleic Acids Based on Target-Induced Shielding Against the Peroxidase-Mimicking Activity of Magnetic Nanoparticles. *Small* (2011) 7(11):1521–5. doi: 10.1002/smll.201001886

9. Asati A, Santra S, Kaittanis C, Nath S, Perez JM. Oxidase-Like Activity of Polymer-Coated Cerium Oxide Nanoparticles. *Angew Chem Int Ed Engl* (2009) 48(13):2308–12. doi: 10.1002/anie.200805279

10. Heckert EG, Karakoti AS, Seal S, Self WT. The Role of Cerium Redox State in the SOD Mimetic Activity of Nanoceria. *Biomaterials* (2008) 29(18):2705–9. doi: 10.1016/j.biomaterials.2008.03.014

11. Song YJ, Wang XH, Zhao C, Qu KG, Ren JS, Qu XG. Label-Free Colorimetric Detection of Single Nucleotide Polymorphism by Using Single-Walled Carbon Nanotube Intrinsic Peroxidase-Like Activity. *Chemistry* (2010) 16(12):3617–21. doi: 10.1002/chem.200902643

12. Pengo P, Polizzi S, Pasquato L, Scrimin P. Carboxylate-Imidazole Cooperativity in Dipeptide-Functionalized Gold Nanoparticles With Esterase-Like Activity. *J Am Chem Soc* (2005) 127(6):1616–7. doi: 10.1021/ja043547c

13. Comotti M, Della Pina C, Matarrese R, Rossi M. The Catalytic Activity of "Naked" Gold Particles. *Angew Chem Int Ed Engl* (2004) 43(43):5812–5. doi: 10.1002/anie.200460446

14. Luo WJ, Zhu CF, Su S, Li D, He Y, Huang Q, et al. Self-Catalyzed, Self-Limiting Growth of Glucose Oxidase-Mimicking Gold Nanoparticles. *ACS Nano* (2010) 4(12):7451–8. doi: 10.1021/nn102592h

15. Song YJ, Qu KG, Zhao C, Ren JS, Qu XG. Graphene Oxide: Intrinsic Peroxidase Catalytic Activity and its Application to Glucose Detection. *Adv Mater* (2010) 22(19):2206–10. doi: 10.1002/adma.200903783

16. Liang MM, Fan KL, Pan Y, Jiang H, Wang F, Yang DL, et al. Fe₃O₄ Magnetic Nanoparticle Peroxidase Mimetic-Based Colorimetric Assay for the Rapid Detection of Organophosphorus Pesticide and Nerve Agent. *Anal Chem* (2013) 85(1):308–12. doi: 10.1021/ac302781r

17. Song YJ, Chen Y, Feng LY, Ren JS, Qu XG. Selective and Quantitative Cancer Cell Detection Using Target-Directed Functionalized Graphene and its Synergetic Peroxidase-Like Activity. *Chem Commun (Camb)* (2011) 47(15):4436–8. doi: 10.1039/c0cc05533f

18. Tao Y, Lin YH, Ren JS, Qu XG. Self-Assembled, Functionalized Graphene and DNA as a Universal Platform for Colorimetric Assays. *Biomaterials* (2013) 34(20):4810–7. doi: 10.1016/j.biomaterials.2013.03.039

19. Xue T, Jiang S, Qu YQ, Su Q, Cheng R, Dubin S, et al. Graphene-Supported Hemin as a Highly Active Biomimetic Oxidation Catalyst. *Angew Chem Int Ed Engl* (2012) 51(16):3822–5. doi: 10.1002/anie.201108400

20. Guo Y, Deng L, Li J, Guo S, Wang E, Dong S. Hemin-Graphene Hybrid Nanosheets With Intrinsic Peroxidase-Like Activity for Label-Free Colorimetric Detection of Single-Nucleotide Polymorphism. *ACS Nano* (2011) 5(2):1282–90. doi: 10.1021/nn1029586

21. Sun HJ, Zhou Y, Ren JS, Qu XG. Carbon Nanozymes: Enzymatic Properties, Catalytic Mechanism, and Applications. *Angew Chem Int Ed Engl* (2018) 57(30):9224–37. doi: 10.1002/anie.201712469

22. Shi WB, Wang QL, Long YJ, Cheng ZL, Chen SH, Zheng HZ, et al. Carbon Nanodots as Peroxidase Mimetics and Their Applications to Glucose Detection. *Chem Commun (Camb)* (2011) 47(23):6695–7. doi: 10.1039/c1cc11943e

23. Zheng XX, Liu Q, Jing C, Li Y, Li D, Luo WJ, et al. Catalytic Gold Nanoparticles for Nanoplasmonic Detection of DNA Hybridization. *Angew Chem Int Ed Engl* (2011) 50(50):11994–8. doi: 10.1002/anie.201105121

24. Liu Z, Tabakman SM, Chen Z, Dai HJ. Preparation of Carbon Nanotube Bioconjugates for Biomedical Applications. *Nat Protoc* (2009) 4(9):1372–82. doi: 10.1038/nprot.2009.146

25. Fan KL, Xi JQ, Fan L, Wang PX, Zhu CH, Tang Y, et al. *In Vivo* Guiding Nitrogen-Doped Carbon Nanozyme for Tumor Catalytic Therapy. *Nat Commun* (2018) 9(1):1440. doi: 10.1038/s41467-018-03903-8

26. Huang YY, Ren JS, Qu XG. Nanozymes: Classification, Catalytic Mechanisms, Activity Regulation, and Applications. *Chem Rev* (2019) 119(6):4357–412. doi: 10.1021/acs.chemrev.8b00672

27. Jiang XX, Liu K, Li Q, Liu M, Yang MH, Chen X. B-Doped Core-Shell Fe@BC Nanozymes: Active Site Identification and Bacterial Inhibition. *Chem Commun (Camb)* (2021) 57(13):1623–6. doi: 10.1039/d0cc06692c

28. Lin YH, Li ZH, Chen ZW, Ren JS, Qu XG. Mesoporous Silica-Encapsulated Gold Nanoparticles as Artificial Enzymes for Self-Activated Cascade Catalysis. *Biomaterials* (2013) 34(11):2600–10. doi: 10.1016/j.biomaterials.2013.01.007

29. Tao Y, Lin YH, Ren JS, Qu XG. A Dual Fluorometric and Colorimetric Sensor for Dopamine Based on BSA-Stabilized Au Nanoclusters. *Biosens Bioelectron* (2013) 42:41–6. doi: 10.1016/j.bios.2012.10.014

30. Lin YH, Zhao AD, Tao Y, Ren JS, Qu XG. Ionic Liquid as an Efficient Modulator on Artificial Enzyme System: Toward the Realization of High-Temperature Catalytic Reactions. *J Am Chem Soc* (2013) 135(11):4207–10. doi: 10.1021/ja400280f

31. Liu Y, Wu HH, Li M, Yin JJ, Nie ZH. pH Dependent Catalytic Activities of Platinum Nanoparticles With Respect to the Decomposition of Hydrogen Peroxide and Scavenging of Superoxide and Singlet Oxygen. *Nanoscale* (2014) 6(20):11904–10. doi: 10.1039/c4nr03848g

32. Fan J, Yin JJ, Ning B, Wu XC, Hu Y, Ferrari M, et al. Direct Evidence for Catalase and Peroxidase Activities of Ferritin-Platinum Nanoparticles. *Biomaterials* (2011) 32(6):1611–8. doi: 10.1016/j.biomaterials.2010.11.004

33. Zhang LB, Laug L, Münchgesang W, Pippel E, Gösele U, Brandsch M, et al. Reducing Stress on Cells With Apoferritin-Encapsulated Platinum Nanoparticles. *Nano Lett* (2010) 10(1):219–23. doi: 10.1021/nl903313r

34. Kotov NA. Chemistry. Inorganic Nanoparticles as Protein Mimics. *Science* (2010) 330(6001):188–9. doi: 10.1126/science.1190094

35. Meng XQ, Li DD, Chen L, He HL, Wang Q, Hong CY, et al. High-Performance Self-Cascade Pyrite Nanozymes for Apoptosis-Ferroptosis Synergistic Tumor Therapy. *ACS Nano* (2021) 15(3):5735–51. doi: 10.1021/acsnano.1c01248

36. Karakoti AS, Singh S, Kumar A, Malinska M, Kuchibhatla SV, Wozniak K, et al. PEGylated Nanoceria as Radical Scavenger With Tunable Redox Chemistry. *J Am Chem Soc* (2009) 131(40):14144–5. doi: 10.1021/ja9051087

37. Asati A, Santra S, Kaittanis C, Perez JM. Surface-Charge-Dependent Cell Localization and Cytotoxicity of Cerium Oxide Nanoparticles. *ACS Nano* (2010) 4(9):5321–31. doi: 10.1021/nn100816s

38. Asati A, Kaittanis C, Santra S, Perez JM. pH-Tunable Oxidase-Like Activity of Cerium Oxide Nanoparticles Achieving Sensitive Fluorigenic Detection of Cancer Biomarkers at Neutral Ph. *Anal Chem* (2011) 83(7):2547–53. doi: 10.1021/ac102826k

39. Chen ZW, Yin JJ, Zhou YT, Zhang Y, Song LN, Song MJ, et al. Dual Enzyme-Like Activities of Iron Oxide Nanoparticles and Their Implication for Diminishing Cytotoxicity. *ACS Nano* (2012) 6(5):4001–12. doi: 10.1021/nn300291r

40. Vallabani NVS, Vinu A, Singh S, Karakoti A. Tuning the ATP-Triggered Pro-Oxidant Activity of Iron Oxide-Based Nanozyme Towards an Efficient Antibacterial Strategy. *J Colloid Interface Sci* (2020) 567:154–64. doi: 10.1016/j.jcis.2020.01.099

41. Gao SS, Lin H, Zhang HX, Yao HL, Chen Y, Shi JL. Nanocatalytic Tumor Therapy by Biomimetic Dual Inorganic Nanozyme-Catalyzed Cascade Reaction. *Adv Sci (Weinh)* (2019) 6(3):1801733. doi: 10.1002/advs. 201801733

42. Singh N, Savanur MA, Srivastava S, D'Silva P, Mugesh G. A Redox Modulatory Mn_3O_4 Nanozyme With Multi-Enzyme Activity Provides Efficient Cytoprotection to Human Cells in a Parkinson's Disease Model. *Angew Chem Int Ed Engl* (2017) 56(45):14267–71. doi: 10.1002/anie. 201708573

43. He WW, Jia HM, Li XX, Lei Y, Li J, Zhao HX, et al. Understanding the Formation of CuS Concave Superstructures With Peroxidase-Like Activity. *Nanoscale* (2012) 4(11):3501–6. doi: 10.1039/c2nr30310h

44. Dutta AK, Das S, Samanta S, Samanta PK, Adhikary B, Biswas P. CuS Nanoparticles as a Mimic Peroxidase for Colorimetric Estimation of Human Blood Glucose Level. *Talanta* (2013) 107:361–7. doi: 10.1016/ j.talanta.2013.01.032

45. Yang ZJ, Cao Y, Li J, Lu MM, Jiang ZK, Hu XY. Smart CuS Nanoparticles as Peroxidase Mimetics for the Design of Novel Label-Free Chemiluminescent Immunoassay. *ACS Appl Mater Interfaces* (2016) 8(19):12031–8. doi: 10.1021/acsami.6b02481

46. Swaidan A, Addad A, Tahon JF, Barras A, Toufaily J, Hamieh T, et al. Ultrasmall $CuS-BSA-Cu_3(PO_4)_2$ Nanozyme for Highly Efficient Colorimetric Sensing of H_2O_2 and Glucose in Contact Lens Care Solutions and Human Serum. *Anal Chim Acta* (2020) 1109:78–89. doi: 10.1016/j.aca.2020.02.064

47. Liang S, Deng XR, Chang Y, Sun CQ, Shao S, Xie ZX, et al. Intelligent Hollow Pt-CuS Janus Architecture for Synergistic Catalysis-Enhanced Sonodynamic and Photothermal Cancer Therapy. *Nano Lett* (2019) 19(6):4134–45. doi: 10.1021/acs.nanolett.9b01595

48. Zhu JL, Peng X, Nie W, Wang YJ, Gao JW, Wen W, et al. Hollow Copper Sulfide Nanocubes as Multifunctional Nanozymes for Colorimetric Detection of Dopamine and Electrochemical Detection of Glucose. *Biosens Bioelectron* (2019) 141:111450. doi: 10.1016/j.bios.2019.111450

49. Huang X, Nan ZD. Porous 2d FeS_2 Nanosheets as a Peroxidase Mimic for Rapid Determination of H_2O_2. *Talanta* (2020) 216:120995. doi: 10.1016/ j.talanta.2020.120995

50. Huang X, Xia F, Nan ZD. Fabrication of FeS_2/SiO_2 Double Mesoporous Hollow Spheres as an Artificial Peroxidase and Rapid Determination of H_2O_2 and Glutathione. *ACS Appl Mater Interfaces* (2020) 12(41):46539–48. doi: 10.1021/acsami.0c12593

51. Liu W, Tian JR, Mao CL, Wang ZF, Liu J, Dahlgren RA, et al. Sulfur Vacancy Promoted Peroxidase-Like Activity of Magnetic Greigite (Fe_3S_4) for Colorimetric Detection of Serum Glucose. *Anal Chim Acta* (2020) 1127:246–55. doi: 10.1016/j.aca.2020.06.056

52. Chen TM, Zou H, Wu XJ, Liu CC, Situ B, Zheng L, et al. Nanozymatic Antioxidant System Based on MoS_2 Nanosheets. *ACS Appl Mater Interfaces* (2018) 10(15):12453–62. doi: 10.1021/acsami.8b01245

53. Ho WJ, Jaffee EM, Zheng L. The Tumour Microenvironment in Pancreatic Cancer-Clinical Challenges and Opportunities. *Nat Rev Clin Oncol* (2020) 17 (9):527–40. doi: 10.1038/s41571-020-0363-5

54. Balachandran VP, Beatty GL, Dougan SK. Broadening the Impact of Immunotherapy to Pancreatic Cancer: Challenges and Opportunities. *Gastroenterology* (2019) 156(7):2056–72. doi: 10.1053/j.gastro.2018.12.038

55. Mittal D, Gubin MM, Schreiber RD, Smyth MJ. New Insights Into Cancer Immunoediting and its Three Component Phases–Elimination, Equilibrium and Escape. *Curr Opin Immunol* (2014) 27:16–25. doi: 10.1016/ j.coi.2014.01.004

56. Shi RC, Tang YQ, Miao HM. Metabolism in Tumor Microenvironment: Implications for Cancer Immunotherapy. *MedComm* (2020) 1(1):47–68. doi: 10.1002/mco2.6

57. Corbet C, Feron O. Tumour Acidosis: From the Passenger to the Driver's Seat. *Nat Rev Cancer* (2017) 17(10):577–93. doi: 10.1038/nrc.2017.77

58. Xu BL, Cui Y, Wang WW, Li SS, Lyu CL, Wang S, et al. Immunomodulation-Enhanced Nanozyme-Based Tumor Catalytic Therapy. *Adv Mater* (2020) 32(33):e2003563. doi: 10.1002/adma.202003563

59. Jing XM, Yang FM, Shao CC, Wei K, Xie MY, Shen H, et al. Role of Hypoxia in Cancer Therapy by Regulating the Tumor Microenvironment. *Mol Cancer* (2019) 18(1):157. doi: 10.1186/s12943-019-1089-9

60. Fokong S, Theek B, Wu Z, Koczera P, Appold L, Jorge S, et al. Image-Guided, Targeted and Triggered Drug Delivery to Tumors Using Polymer-Based Microbubbles. *J Control Release* (2012) 163(1):75–81. doi: 10.1016/ j.jconrel.2012.05.007

61. Lee AL, Wang Y, Cheng HY, Pervaiz S, Yang YY. The Co-Delivery of Paclitaxel and Herceptin Using Cationic Micellar Nanoparticles. *Biomaterials* (2009) 30(5):919–27. doi: 10.1016/j.biomaterials.2008.10.062

62. Zhang LN, Deng HH, Lin FL, Xu XW, Weng SH, Liu AL, et al. *In Situ* Growth of Porous Platinum Nanoparticles on Graphene Oxide for Colorimetric Detection of Cancer Cells. *Anal Chem* (2014) 86(5):2711–8. doi: 10.1021/ac404104j

63. Qu F, Li T, Yang M. Colorimetric Platform for Visual Detection of Cancer Biomarker Based on Intrinsic Peroxidase Activity of Graphene Oxide. *Biosens Bioelectron* (2011) 26(9):3927–31. doi: 10.1016/j.bios.2011.03.013

64. Loynachan CN, Soleimany AP, Dudani JS, Lin Y, Najer A, Bekdemir A, et al. Renal Clearable Catalytic Gold Nanoclusters for *In Vivo* Disease Monitoring. *Nat Nanotechnol* (2019) 14(9):883–90. doi: 10.1038/s41565-019-0527-6

65. Fan KL, Cao CQ, Pan YX, Lu D, Yang DL, Feng J, et al. Magnetoferritin Nanoparticles for Targeting and Visualizing Tumour Tissues. *Nat Nanotechnol* (2012) 7(7):459–64. doi: 10.1038/nnano.2012.90

66. Huang SX, Li JF, Han L, Liu SH, Ma HJ, Huang RQ, et al. Dual Targeting Effect of Angiopep-2-Modified, DNA-Loaded Nanoparticles for Glioma. *Biomaterials* (2011) 32(28):6832–8. doi: 10.1016/j.biomaterials.2011.05.064

67. Xin HL, Jiang XY, Gu JJ, Sha XY, Chen LC, Law K, et al. Angiopep-Conjugated Poly(Ethylene Glycol)-Co-Poly(ε-Caprolactone) Nanoparticles as Dual-Targeting Drug Delivery System for Brain Glioma. *Biomaterials* (2011) 32(18):4293–305. doi: 10.1016/j.biomaterials.2011.02.044

68. Rhee SG. Cell Signaling. H_2O_2, a Necessary Evil for Cell Signaling. *Science* (2006) 312(5782):1882–3. doi: 10.1126/science.1130481

69. Zhang K, Kaufman RJ. From Endoplasmic-Reticulum Stress to the Inflammatory Response. *Nature* (2008) 454(7203):455–62. doi: 10.1038/ nature07203

70. Yang F, Hu SL, Zhang Y, Cai XW, Huang Y, Wang F, et al. A Hydrogen Peroxide-Responsive O_2 Nanogenerator for Ultrasound and Magnetic-Resonance Dual Modality Imaging. *Adv Mater* (2012) 24(38):5205–11. doi: 10.1002/adma.201202367

71. Zhang W, Hu SL, Yin JJ, He WW, Lu W, Ma M, et al. Prussian Blue Nanoparticles as Multienzyme Mimetics and Reactive Oxygen Species Scavengers. *J Am Chem Soc* (2016) 138(18):5860–5. doi: 10.1021/ jacs.5b12070

72. Dou Y, Li X, Yang WT, Guo YY, Wu ML, Liu YJ, et al. PB@Au Core-Satellite Multifunctional Nanotheranostics for Magnetic Resonance and Computed Tomography Imaging *In Vivo* and Synergetic Photothermal and Radiosensitive Therapy. *ACS Appl Mater Interfaces* (2017) 9(2):1263–72. doi: 10.1021/acsami.6b13493

73. Wang X, Niu DC, Li P, Wu Q, Bo XW, Liu BJ, et al. Dual-Enzyme-Loaded Multifunctional Hybrid Nanogel System for Pathological Responsive Ultrasound Imaging and T2-Weighted Magnetic Resonance Imaging. *ACS Nano* (2015) 9(6):5646–56. doi: 10.1021/nn5068094

74. Ragg R, Schilmann AM, Korschelt K, Wieseotte C, Kluenker M, Viel M, et al. Intrinsic Superoxide Dismutase Activity of MnO Nanoparticles Enhances the Magnetic Resonance Imaging Contrast. *J Mater Chem B* (2016) 4 (46):7423–8. doi: 10.1039/c6tb02078j

75. Wang ZZ, Zhang Y, Ju EG, Liu Z, Cao FF, Chen ZW, et al. Biomimetic Nanoflowers by Self-Assembly of Nanozymes to Induce Intracellular Oxidative Damage Against Hypoxic Tumors. *Nat Commun* (2018) 9 (1):3334. doi: 10.1038/s41467-018-05798-x

76. Yao J, Cheng Y, Zhou M, Zhao S, Lin SC, Wang X, et al. ROS Scavenging Mn_3O_4 Nanozymes for *In Vivo* Anti-Inflammation. *Chem Sci* (2018) 9 (11):2927–33. doi: 10.1039/c7sc05476a

77. Li XS, Lovell JF, Yoon J, Chen XY. Clinical Development and Potential of Photothermal and Photodynamic Therapies for Cancer. *Nat Rev Clin Oncol* (2020) 17(11):657–74. doi: 10.1038/s41571-020-0410-2

78. Qian CG, Yu JC, Chen YL, Hu QY, Xiao XZ, Sun WJ, et al. Light-Activated Hypoxia-Responsive Nanocarriers for Enhanced Anticancer Therapy. *Adv Mater* (2016) 28(17):3313–20. doi: 10.1002/adma.201505869

79. Tong X, Srivatsan A, Jacobson O, Wang Y, Wang ZT, Yang XY, et al. Monitoring Tumor Hypoxia Using ^{18}F-FMISO PET and Pharmacokinetics

Modeling After Photodynamic Therapy. *Sci Rep* (2016) 6:31551. doi: 10.1038/srep31551

80. Lu KD, He CB, Guo NN, Chan C, Ni KY, Weichselbaum RR, et al. Chlorin-Based Nanoscale Metal-Organic Framework Systemically Rejects Colorectal Cancers *via* Synergistic Photodynamic Therapy and Checkpoint Blockade Immunotherapy. *J Am Chem Soc* (2016) 138(38):12502–10. doi: 10.1021/jacs.6b06663

81. Zhang Y, Wang FM, Liu CQ, Wang ZZ, Kang LH, Huang YY, et al. Nanozyme Decorated Metal-Organic Frameworks for Enhanced Photodynamic Therapy. *ACS Nano* (2018) 12(1):651–61. doi: 10.1021/acsnano.7b07746

82. Jiang YY, Li JC, Zeng ZL, Xie C, Lyu Y, Pu KY. Organic Photodynamic Nanoinhibitor for Synergistic Cancer Therapy. *Angew Chem Int Ed Engl* (2019) 58(24):8161–5. doi: 10.1002/anie.201903968

83. Liu CP, Wu TH, Liu CY, Chen KC, Chen YX, Chen GS, et al. Self-Supplying O₂ Through the Catalase-Like Activity of Gold Nanoclusters for Photodynamic Therapy Against Hypoxic Cancer Cells. *Small* (2017) 13 (26):1–9. doi: 10.1002/smll.201700278

84. Yang Y, Zhu DM, Liu Y, Jiang B, Jiang W, Yan XY, et al. Platinum-Carbon-Integrated Nanozymes for Enhanced Tumor Photodynamic and Photothermal Therapy. *Nanoscale* (2020) 12(25):13548–57. doi: 10.1039/d0nr02800b

85. Liu S, Pan XT, Liu HY. Two-Dimensional Nanomaterials for Photothermal Therapy. *Angew Chem Int Ed Engl* (2020) 59(15):5890–900. doi: 10.1002/anie.201911477

86. Liu JJ, Yang Y, Zhu WW, Yi X, Dong ZL, Xu XN, et al. Nanoscale Metal-Organic Frameworks for Combined Photodynamic & Radiation Therapy in Cancer Treatment. *Biomaterials* (2016) 97:1–9. doi: 10.1016/j.biomaterials.2016.04.034

87. Liu C, Xing J, Akakuru OU, Luo LJ, Sun S, Zou RF, et al. Nanozymes-Engineered Metal-Organic Frameworks for Catalytic Cascades-Enhanced Synergistic Cancer Therapy. *Nano Lett* (2019) 19(8):5674–82. doi: 10.1021/acs.nanolett.9b02253

88. Dong SM, Dong YS, Jia T, Liu SK, Liu J, Yang D, et al. GSH-Depleted Nanozymes With Hyperthermia-Enhanced Dual Enzyme-Mimic Activities for Tumor Nanocatalytic Therapy. *Adv Mater* (2020) 32(42):e2002439. doi: 10.1002/adma.202002439

89. Li ZH, Chen Y, Sun YY, Zhang XZ. Platinum-Doped Prussian Blue Nanozymes for Multiwavelength Bioimaging Guided Photothermal Therapy of Tumor and Anti-Inflammation. *ACS Nano* (2021) 15(3):5189–200. doi: 10.1021/acsnano.0c10388

90. Son SB, Kim JH, Wang XW, Zhang CL, Yoon SA, Shin JW, et al. Multifunctional Sonosensitizers in Sonodynamic Cancer Therapy. *Chem Soc Rev* (2020) 49(11):3244–61. doi: 10.1039/c9cs00648f

91. Zhu P, Chen Y, Shi JL. Nanoenzyme-Augmented Cancer Sonodynamic Therapy by Catalytic Tumor Oxygenation. *ACS Nano* (2018) 12(4):3780–95. doi: 10.1021/acsnano.8b00999

92. Liang S, Deng XR, Ma PA, Cheng ZY, Lin J. Recent Advances in Nanomaterial-Assisted Combinational Sonodynamic Cancer Therapy. *Adv Mater* (2020) 32(47):e2003214. doi: 10.1002/adma.202003214

93. Sun D, Pang X, Cheng Y, Ming J, Xiang SJ, Zhang C, et al. Ultrasound-Switchable Nanozyme Augments Sonodynamic Therapy Against Multidrug-Resistant Bacterial Infection. *ACS Nano* (2020) 14(2):2063–76. doi: 10.1021/acsnano.9b08667

94. An J, Hu YG, Cheng K, Li C, Hou XL, Wang GL, et al. ROS-Augmented and Tumor-Microenvironment Responsive Biodegradable Nanoplatform for Enhancing Chemo-Sonodynamic Therapy. *Biomaterials* (2020) 234:119761. doi: 10.1016/j.biomaterials.2020.119761

95. Li GZ, Wang SP, Deng DS, Xiao ZS, Dong ZL, Wang ZP, et al. Fluorinated Chitosan to Enhance Transmucosal Delivery of Sonosensitizer-Conjugated Catalase for Sonodynamic Bladder Cancer Treatment Post-Intravesical Instillation. *ACS Nano* (2020) 14(2):1586–99. doi: 10.1021/acsnano.9b06689

96. Wang XW, Zhong XY, Bai LX, Xu J, Gong F, Dong ZL, et al. Ultrafine Titanium Monoxide (TiO₁₊ₓ) Nanorods for Enhanced Sonodynamic Therapy. *J Am Chem Soc* (2020) 142(14):6527–37. doi: 10.1021/jacs.9b10228

97. Zhang C, Zhao KL, Bu WB, Ni DL, Liu YY, Feng JW, et al. Marriage of Scintillator and Semiconductor for Synchronous Radiotherapy and Deep

98. Photodynamic Therapy With Diminished Oxygen Dependence. *Angew Chem Int Ed Engl* (2015) 54(6):1770–4. doi: 10.1002/anie.201408472

98. Song GS, Cheng L, Chao Y, Yang K, Liu Z. Emerging Nanotechnology and Advanced Materials for Cancer Radiation Therapy. *Adv Mater* (2017) 29 (32):1–26. doi: 10.1002/adma.201700996

99. Fan WP, Shen B, Bu WB, Chen F, Zhao KL, Zhang SJ, et al. Rattle-Structured Multifunctional Nanotheranostics for Synergetic Chemo-/Radiotherapy and Simultaneous Magnetic/Luminescent Dual-Mode Imaging. *J Am Chem Soc* (2013) 135(17):6494–503. doi: 10.1021/ja312225b

100. Xiao QF, Zheng XP, Bu WB, Ge WQ, Zhang SJ, Chen F, et al. A Core/Satellite Multifunctional Nanotheranostic for *In Vivo* Imaging and Tumor Eradication by Radiation/Photothermal Synergistic Therapy. *J Am Chem Soc* (2013) 135(35):13041–8. doi: 10.1021/ja404985w

101. Fan WP, Bu WB, Zhang Z, Shen B, Zhang H, He QJ, et al. X-Ray Radiation-Controlled NO-Release for on-Demand Depth-Independent Hypoxic Radiosensitization. *Angew Chem Int Ed Engl* (2015) 54(47):14026–30. doi: 10.1002/anie.201504536

102. Prasad P, Gordijo CR, Abbasi AZ, Maeda A, Ip A, Rauth AM, et al. Multifunctional Albumin-MnO₂ Nanoparticles Modulate Solid Tumor Microenvironment by Attenuating Hypoxia, Acidosis, Vascular Endothelial Growth Factor and Enhance Radiation Response. *ACS Nano* (2014) 8(4):3202–12. doi: 10.1021/nn405773r

103. Gordijo CR, Shuhendler AJ, Wu XY. Glucose-Responsive Bioinorganic Nanohybrid Membrane for Self-Regulated Insulin Release. *Adv Funct Mater* (2010) 20(9):1404–12. doi: 10.1002/adfm.200901581

104. Yi X, Chen L, Zhong XY, Gao RL, Qian YT, Wu F, et al. Core–shell Au@MnO₂ Nanoparticles for Enhanced Radiotherapy *via* Improving the Tumor Oxygenation. *Nano Res* (2016) 9(11):3267–78. doi: 10.1007/s12274-016-1205-8

105. Zhang C, Bu WB, Ni DL, Zhang SJ, Li Q, Yao ZW, et al. Synthesis of Iron Nanometallic Glasses and Their Application in Cancer Therapy by a Localized Fenton Reaction. *Angew Chem Int Ed Engl* (2016) 55(6):2101–6. doi: 10.1002/anie.201510031

106. Alili L, Sack M, Karakoti AS, Teuber S, Puschmann K, Hirst SM, et al. Combined Cytotoxic and Anti-Invasive Properties of Redox-Active Nanoparticles in Tumor-Stroma Interactions. *Biomaterials* (2011) 32 (11):2918–29. doi: 10.1016/j.biomaterials.2010.12.056

107. Lin WS, Huang YW, Zhou XD, Ma Y. Toxicity of Cerium Oxide Nanoparticles in Human Lung Cancer Cells. *Int J Toxicol* (2006) 25 (6):451–7. doi: 10.1080/10915810600959543

108. Zhu XF, Gong YC, Liu YN, Yang CH, Wu SJ, Yuan GL, et al. Ru@CeO₂ Yolk Shell Nanozymes: Oxygen Supply *in Situ* Enhanced Dual Chemotherapy Combined With Photothermal Therapy for Orthotopic/Subcutaneous Colorectal Cancer. *Biomaterials* (2020) 242:119923. doi: 10.1016/j.biomaterials.2020.119923

109. Li SS, Shang L, Xu BL, Wang SH, Gu K, Wu QY, et al. A Nanozyme With Photo-Enhanced Dual Enzyme-Like Activities for Deep Pancreatic Cancer Therapy. *Angew Chem Int Ed Engl* (2019) 58(36):12624–31. doi: 10.1002/anie.201904751

110. Yang X, Yang Y, Gao F, Wei JJ, Qian CG, Sun MJ. Biomimetic Hybrid Nanozymes With Self-Supplied H⁺ and Accelerated O₂ Generation for Enhanced Starvation and Photodynamic Therapy Against Hypoxic Tumors. *Nano Lett* (2019) 19(7):4334–42. doi: 10.1021/acs.nanolett.9b00934

111. Zhang A, Pan SJ, Zhang YH, Chang J, Cheng J, Huang ZC, et al. Carbon-Gold Hybrid Nanoprobes for Real-Time Imaging, Photothermal/Photodynamic and Nanozyme Oxidative Therapy. *Theranostics* (2019) 9 (12):3443–58. doi: 10.7150/thno.33266

112. Wang M, Chang MY, Chen Q, Wang DM, Li CX, Hou ZY, et al. Au₂Pt-PEG-Ce6 Nanoformulation With Dual Nanozyme Activities for Synergistic Chemodynamic Therapy/Phototherapy. *Biomaterials* (2020) 252:120093. doi: 10.1016/j.biomaterials.2020.120093

113. Li Y, Yun KH, Lee H, Goh SH, Suh YG, Choi Y. Porous Platinum Nanoparticles as a High-Z and Oxygen Generating Nanozyme for Enhanced Radiotherapy *In Vivo*. *Biomaterials* (2019) 197:12–9. doi: 10.1016/j.biomaterials.2019.01.004

114. Wang DD, Wu HH, Phua SZF, Yang GB, Qi LW, Gu L, et al. Self-Assembled Single-Atom Nanozyme for Enhanced Photodynamic Therapy Treatment of Tumor. *Nat Commun* (2020) 11(1):357. doi: 10.1038/s41467-019-14199-7